J. Biomed. Eng. Res : 154-163, 2006

# A Low-noise Multichannel Magnetocardiogram System for the Diagnosis of Heart Electric Activity

Yong-Ho Lee, Kiwoong Kim, Jin-Mok Kim, Hyukchan Kwon,
Kwon-Kyu Yu, In-Seon Kim, Yong-Ki Park

*Bio-signal Research Center, Korea Research Institute of Standards and Science*

*(Received March 27, 2006. Accepted July 28, 2006)*

**Abstract**

A 64-channel magnetocardiogram (MCG) system using low-noise superconducting quantum interference device (SQUID) planar gradiometers was developed for the measurements of cardiac magnetic fields generated by the heart electric activity. Owing to high flux-to-voltage transfers of double relaxation oscillation SQUID (DROS) sensors, the flux-locked loop electronics for SQUID operation could be made simpler than that of conventional DC SQUIDs, and the SQUID control was done automatically through a fiber-optic cable. The pickup coils are first-order planar gradiometers with a baseline of 4 cm. The insert has 64 planar gradiometers as the sensing channels and were arranged to measure MCG field components tangential to the chest surface. When the 64-channel insert was in operation everyday, the average boil-off rate of the dewar was 3.6 L/d. The noise spectrum of the SQUID planar gradiometer system was about 5 $fT_{rms}/\sqrt{Hz}$ at 100 Hz, operated inside a moderately shielded room. The MCG measurements were done at a sampling rate of 500 Hz or 1 kHz, and realtime display of MCG traces and heart rate were displayed. After the acquisition, magnetic field mapping and current mapping could be done. From the magnetic and current information, parameters for the diagnosis of myocardial ischemia were evaluated to be compared with other diagnostic methods.

**Key words** : SQUID, magnetocardiogram, multichannel system, heart disease

## I. INTRODUCTION

Magnetocardiography (MCG) is the magnetic field signals generated by the electrophysiological activity of heart muscles. MCG has many merits over the electrocardiography(ECG); the MCG is more sensitive to tangential currents, vortex currents, and the current flow between the endocardium and the epicardium. In addition, MCG measurement is less dependent on the variation in electrical conductivity of the medium around the heart and is non-contact method [1, 2]. Recently, it was proven that myocardial ischemia could be detected by MCG with a high diagnostic accuracy: positive predictive value of 91.2 % and negative predictive value of 96.2 % [3-5].

In order to measure time varying cardiac magnetic fields reliably, we need a multichannel system with number of sensors sufficient enough to get the major field distribution in a short time. Up to now, several MCG systems were developed with sensing channel numbers of 4 or 9 to scan the chest by moving the patient bed several times, or number of channels around 60 which have sensor coverage areas large enough to measure MCG field distributions in a single position measurement [6]. Conventional MCG systems have sensor distribution to measure magnetic field component normal to the chest surface. When we measure normal component of MCG fields, we get two magnetic field peaks of opposite polarity for a given current source. Therefore, the sensor coverage area becomes large, increasing the inner and also the outer diameter of the dewar at the tail part. Increased dewar inner diameter increases the boil-off rate of liquid He, and the increased outer diameter can hit the chins of patients of a short height or children.

If we measure magnetic field components tangential to the chest surface, we get a main field peak directly above the current source, and a smaller sensor coverage area than that of the normal measurement can provide the major field distribution. And thus dewar inner tail diameter can be made smaller, which can lower the boil-off rate of the liquid helium dewar compared with the normal component measurement systems. In order to develop an MCG system with low-boil off rate, we designed and fabricated an MCG system measuring tangential components of MCG signals.

Corresponding Author : Yong-Ho Lee,
Bio-signal Research Center, Korea Research Institute of Standards and Science, 1 Doryong, Yuseong, Daejeon, 305-340, Korea
Tel : +82-42-868-5235 / Fax : +82-42-868-5290
E-mail : yhlee@kriss.re.kr

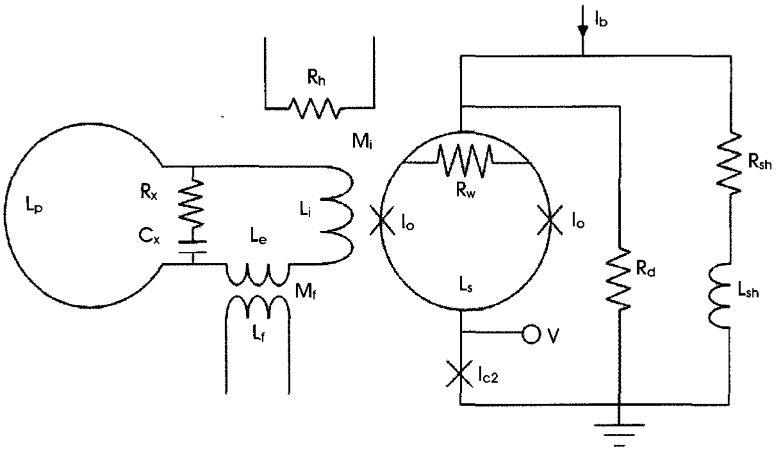


Fig. 1. Schematic circuit diagram of the DROS planar gradiometer.

As a clinical diagnostic device, the signal-to-noise ratio (SNR) of MCG traces would be most important to provide accurate analysis results. SNR is determined by the sensitivity of the SQUID system which includes SQUIDs, electronics and dewar, and by the combined noise rejection performance of the shielded room, gradiometric pickup coil and signal processing. To make low-noise magnetic field sensors with the function of environmental noise rejection, we fabricated SQUID planar gradiometers with high intrinsic balancing. The SQUIDs have large flux-to-voltage transfers by using double relaxation oscillation SQUID (DROS) scheme, and thus simple flux-locked loop electronics with preamplifiers of modest input voltage noise can be used to measure SQUID output voltages.

In this paper, we report a multichannel MCG system with low-noise planar gradiometers arranged to measure tangential components of cardiac fields. The design, construction, and operation characteristics of the MCG system were described.

## II. MATERIALS AND METHODS

### A. Fabrication of SQUID Planar Gradiometer

Since the amplitudes of MCG signals are weak, in the range of 1-10 pT, we need sensitive magnetic sensors using low-noise SQUIDs. On the other hands, the MCG signals are much weaker than earth's dc magnetic field strength or environmental noises. In order to realize a low-noise magnetic sensor with the function of noise rejection, we designed and fabricated an SQUID planar gradiometer consisted of an SQUID as the flux-to-voltage converter and a gradiometric thin film coil. In addition, we adopted the DROS with large flux-to-voltage transfer coefficients to simplify the readout electronics of SQUIDs.

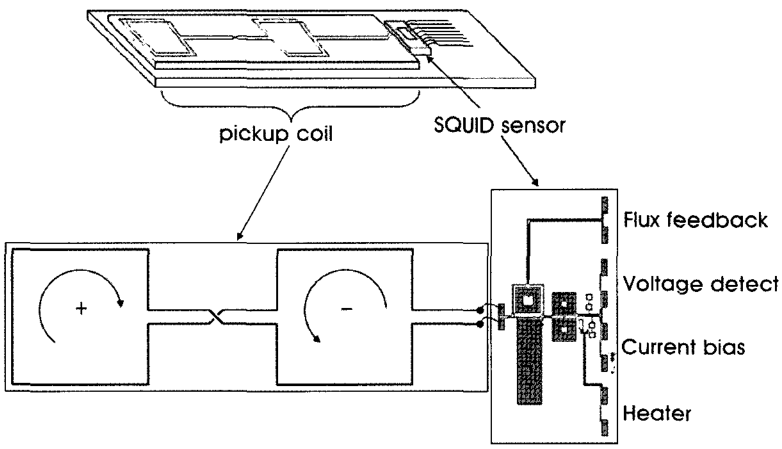


Fig. 2. Assembled structure of the planar pickup coil and SQUID sensor in a printed circuit board.

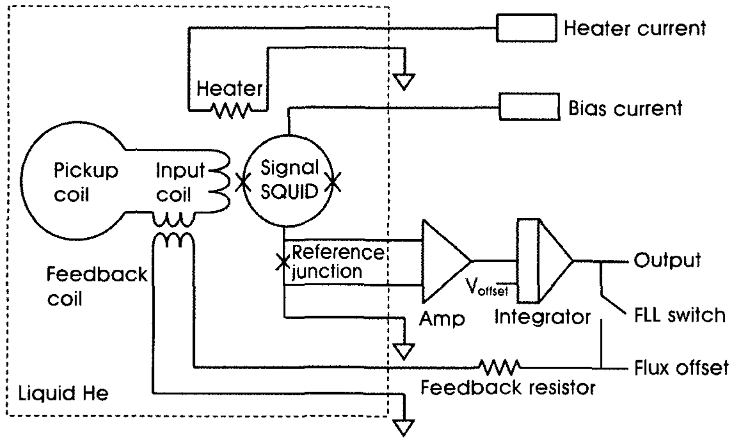


Fig. 3. Schematic circuit diagram of the FLL electronics.

The DROS sensor consists of a signal SQUID and a reference junction, shunted by a relaxation circuit of a resistor and an inductor, as shown in figure 1 [7, 8]. In a dc bias current, the DROS functions as the comparator of two critical currents, the critical current of the signal SQUID and that of the reference junction. If the critical current of the signal SQUID is larger than that of the reference junction, there appears voltage across the reference junction. In the opposite case, no voltage signal is generated. If the flux to the signal SQUID is changed such that the two critical currents compete in magnitude, the output voltage changes abruptly, resulting in a large flux-to-voltage transfer coefficient.

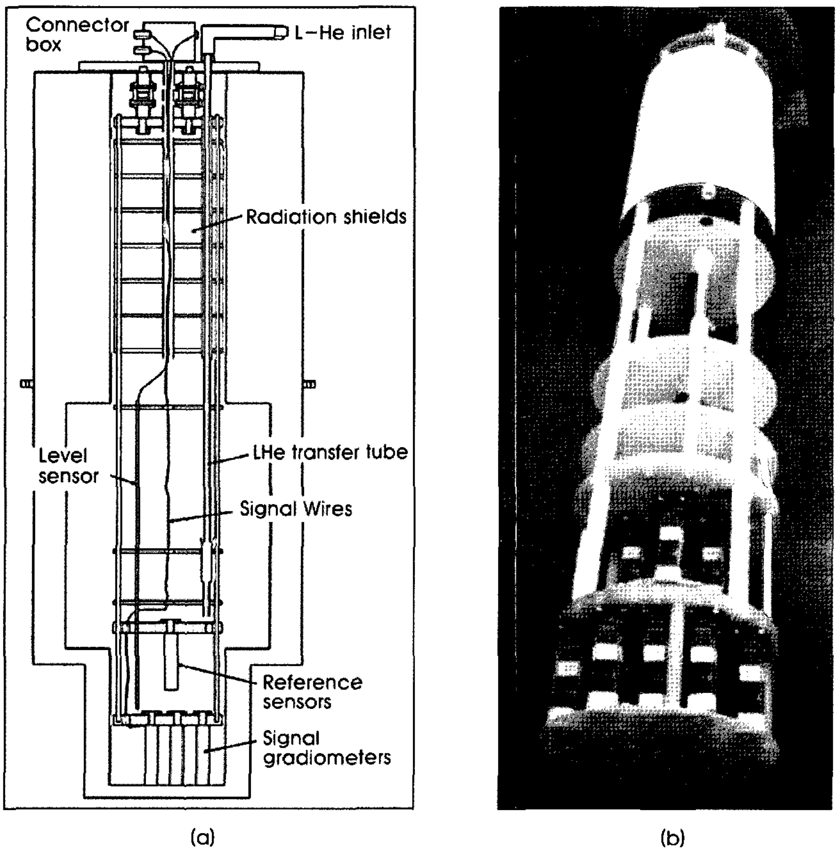


Fig. 4. SQUID insert. (a) Structure of the insert installed inside the dewar and (b) photograph of the insert.

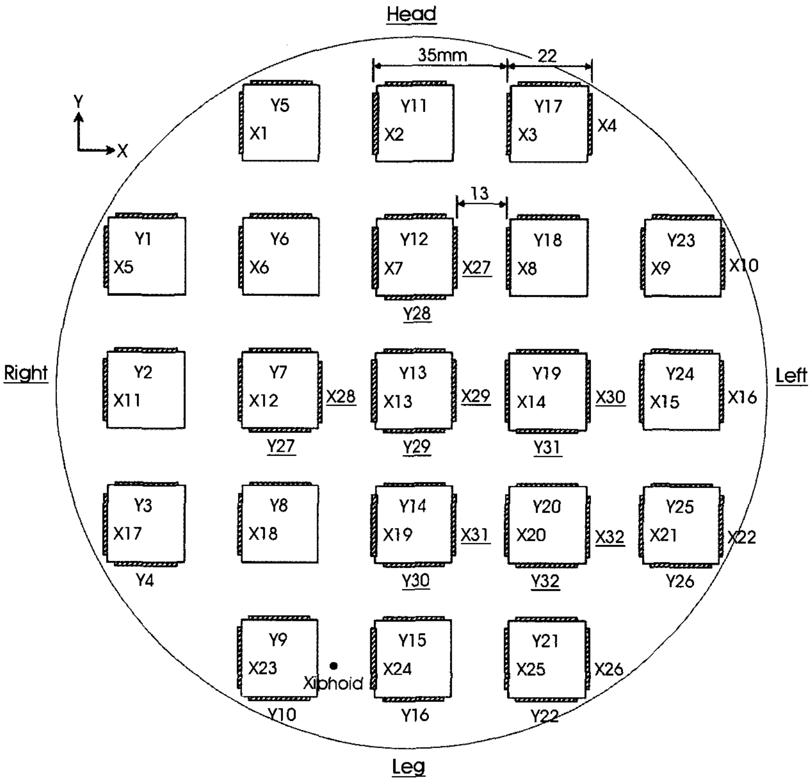


Fig. 5. Arrangement of the 64 planar gradiometers. 32 planar gradiometers measure x-component of the MCG signals and the other 32 measure y-component.

The structure of the DROS planar gradiometer is shown in figure 2. The pickup coil is a series-connected first-order gradiometer with a baseline of 40 mm. The two coils, proximal coil and distal coil are wound in opposite direction with a figure of "8" structure to cancel uniform background field noises. In order to improve the productivity of fabrication, the pickup coils and DROS sensors were fabricated on separate wafers, and were mounted on printed circuit boards (PCBs) which has a size of 16 mm × 78 mm. Details of the device parameters can be found elsewhere [9].

The DROS sensors were fabricated using Nb/$AlO_x$/Nb Josephson junction technology with the following 4-level process: deposition of Nb/$AlO_x$/Nb trilayer by dc magnetron sputtering, definition of Josephson junctions by reactive ion etching, insulation using $SiO_2$ thin film by plasma-enhanced chemical vapor deposition, deposition of Pd resistor by dc magnetron sputtering and deposition of Nb wiring by dc magnetron sputtering. The pickup coils were fabricated on 4-inch Si wafers using the following fabrication sequence: deposition of Nb bottom line, insulation using $SiO_2$ thin film and deposition of Nb wiring. All the thin film layers were patterned using the lift-off method. The superconductive connection between the pickup coil and the input coil of the DROS sensor was done by an ultrasonic bonding of Nb wires using vacuum annealed Nb wires. Both the Nb wires and Al wires were bonded using an ultrasonic wedge bonding method. To remove any trapped flux in the SQUID and flux transformer, a heating resistor of 100 Ω was formed in a close distance from the SQUID, with a meander structure to reduce magnetic noises from the heater.

### B. SQUID Electronics

In order to operate the DROS planar gradiometer in the flux-locked loop (FLL) mode, we need 3 pairs of lines, with each pair for the dc bias current, voltage readout and flux feedback, respectively. Including two lines for the heater, 8 lines or 4 pairs are needed for each channel. The fabricated DROSs had modulation voltages of 80~100$\mu$V, and the flux-to-voltage transfers $dV/d\Phi$ were about 1 mV/$\Phi_0$, at around mid point of the modulation voltage.

The schematic diagram of the FLL circuit is shown in figure 3. If a preamplifier having an input voltage noise value $V_n$ is connected to an SQUID with $dV/d\Phi$, the equivalent flux noise of the preamplifier is given by $V_n/(dV/d\Phi)$. Ordinary preamplifiers using low-noise operational amplifiers of bipolar type have an input voltage noise of about 1 nV/$\sqrt{}$Hz or larger in the white region. If we connect these preamplifiers to dc SQUIDs with typical $dV/d\Phi$ values of 100 $\mu$V/$\Phi_0$, the equivalent flux noises

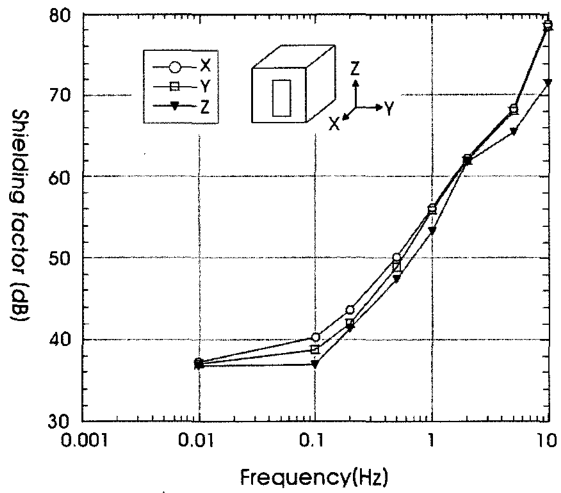


Fig. 6. Shielding factors as a function of frequency for three directions.

of these preamplifiers are about 10 $\mu\Phi_0/\sqrt{Hz}$. These values are larger than the flux noises of ordinary dc SQUIDs, and thus sensitivities of dc SQUIDs become preamplifier limited.

In the present study, the preamplifiers were fabricated using common LT1128 operational amplifiers (Linear Technology). The input voltage noises of the preamplifiers were about 1.5 $nV/\sqrt{Hz}$ at 100 Hz. For a typical flux-to-voltage transfer of 1 $mV/\Phi_0$, the equivalent flux noise of the preamplifier is 1.5 $\mu\Phi_0/\sqrt{Hz}$ at 100 Hz, which is negligible compared to the average flux noise of DROS planar gradiometers (5.8 $\mu_0$/Hz at 100 Hz). Represented as the flux noise power (square of the flux noise), the preamplifier contributes about 7 % to the total noise of the SQUID system.

16 FLL printed circuit boards (PCBs) were assembled in parallel in one aluminum box, and 4 boxes for 64 the channels were installed on top of the dewar gantry. The FLL outputs were passed through the analog signal processing (ASP) electronics, consisted of 16 PCBs and enter into the A/D card of the computer. Each ASP PCB has 4-channel ASP circuits and the ASP electronics were mounted in a single 19-inch sub-rack, outside of the magnetically-shielded room. In order to control the FLL operations and ASP settings, digital pulses were used through a fiber-optic cable. The ASP circuits have high-pass filters (0.1 Hz), amplifiers (100 times), low-pass filters (100 Hz) and 60-Hz notch filters [10].

### C. 64-channel SQUID Insert and Dewar

The 64-channel insert consists of epoxy blocks for planar gradiometer, signal wires, a level meter, radiation shields (baffles), and a connector box, etc, as shown in figure 4. The planar gradiometers at the tail part have 21 long rectangular holders and each holder has 2~4 planar gradiometers. Figure 5 shows the arrangement of 64 planar gradiometers. The standard distance between adjacent parallel gradiometers is

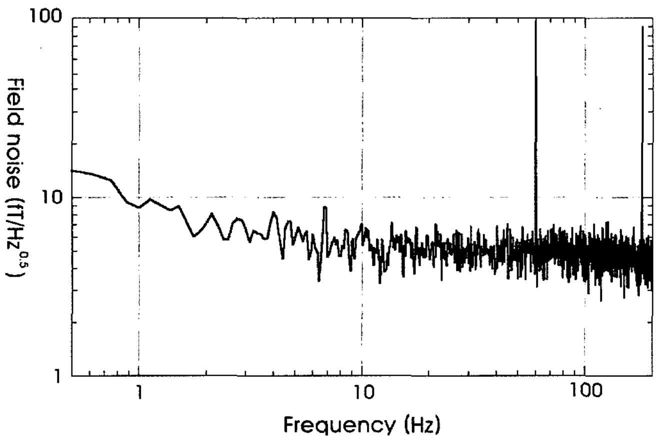


Fig. 7. Noise spectrum of a DROS planar gradiometer, measured inside a magnetically shielded room.

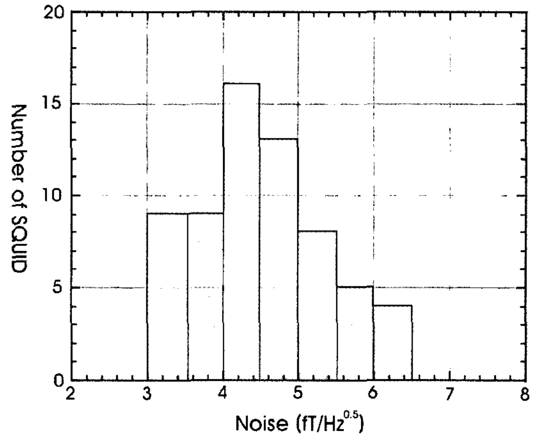


**Fig. 8.** Histogram of the noise distribution for the 64 channels. The average noise value of the 64 channels is 5 $fT_{rms}/\sqrt{Hz}$ at 100 Hz.

35 mm. The 64-channel insert was designed to measure field components tangential to the chest surface; $dB_x/dz$ and $dB_y/dz$, where z-axis is normal to the chest surface. Tangential gradiometers measuring off-diagonal components of the field gradient matrix has a magnetic field peak just above the current dipole when the pickup coil plane is arranged parallel to the dipole direction. Thus, it is possible to get the essential field distribution with a sensor coverage area smaller than the normal measurements. The senor coverage area of the 64-channel is 162 mm×162 mm, which seems to be insufficient compared to the conventional MCG systems measuring the normal component. However, a simulation study showed that tangential measurements can localize current dipoles with a confidence region diameter larger than the normal measurement for the same localization error [11]. In addition to the 64 sensing channels, 8 reference planar gradiometers were mounted at 16 cm above the sensing channels to pickup background noises and to apply the adaptive filtering in case of very noisy environments.

To minimize thermal load, low-thermal-conductivity manganin wires of 127 m diameter were used for all the signal lines. Since the average electrical resistance of the manganin wire between 300 K and 4.2 K is about 40 Ω/m, and the input current noise of LT1128 is 2 pA/$\sqrt{}$Hz at 100 Hz, the voltage noise due to the wire resistance is about 80 pV/$\sqrt{}$Hz at 100 Hz. This noise level is negligible compared with the input voltage noise of LT1128 (1.5 nV/$\sqrt{}$Hz). All the wires were twisted in pair to eliminate magnetic coupling.

The mechanical support between the SQUID planar gradiometer assembly and the room-temperature were made of low-thermal-conductivity fiber-reinforced plastic (FRP) tubes which has low thermal conductivity and high mechanical strength. The radiation baffles, made of multiple layers of Cu-PCB and styrofoam, were used to shield the heat coming from the dewar neck. The cold evaporating gas was used to cool the signal lines and the upper part of the insert. To compensate a

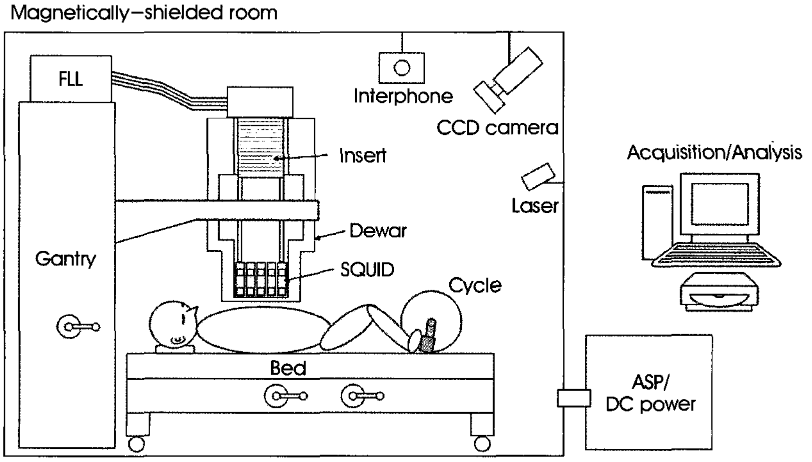


**Fig. 9.** Block diagram of the MCG system.

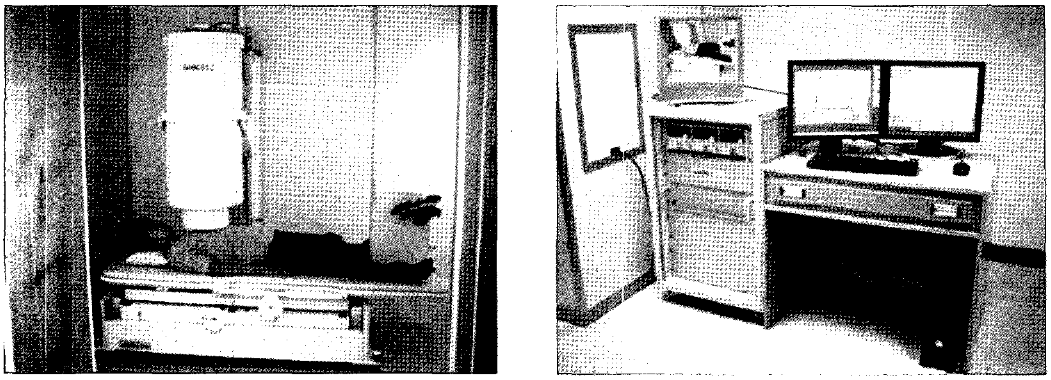

(a) (b)

Fig. 10. Photograph of the MCG system. (a) Part of the system inside the MSR with FLL electronics, dewar and bed. (b) ASP and software installed outside the MSR.

dimensional change caused by thermal contraction of the insert on cooling, a sliding mechanism and spring were used which ensure the insert tail touches the dewar bottom all the time.

### D. Liquid He Dewar

The He dewar was fabricated from FRP tubes, multiple layers of superinsulation (SI) and polyester net. The SI has 25-nm thick Al films on both sides of Mylar substrate. In order to reduce eddy current noises from the thermal motion of electrons in the Al films, the Al films having an island structure were used with an island size of about 10 mm × 10 mm. The heat collected in the SI layers was cooled by using thermal shields anchored on the neck tube. The thermal shields were made from Cu wires woven in the form of a coil foil to minimize thermal noises. The FRP tubes and FRP plates were glued each other using a 2850-FT stycast. To increase the vacuum holding time of the dewar vacuum, a cryogenic getter using charcoal granules were attached at the cold tail part of the inner FRP tube.

The main reservoir of the dewar has an inner diameter of 334 mm and a length of 385 mm. The flat tail has an inner tail diameter of 192 mm, and the distance between the liquid helium and the room temperature is 20 mm. The liquid capacity of the main reservoir is 34 L and the tail volume is 6 L. When the 64-channel is in everyday operation, the average boil-off rate of the dewar is 3.6 L/d. Once the dewar is filled up, the liquid level drops to 15 L in a week. Though a liquid volume of 3 L is the minimum necessary volume to operate the 64 planar gradiometers, we refill the dewar once a week with a refill volume of 25 L.

### E. Magnetically Shielded Room

In order to ensure good signal-to-noise ratios of MCG signals, a magnetically-shielded room (MSR) was fabricated. The internal and external dimensions of the MSR are 2.4 m (W) × 2.4 m (L) × 2.4 m (H) and 2.8 m (W) × 2.8 m (L) ×2.8 m (H), respectively. The MSR was fabricated from high permeability Mu-metal sheets and high conductivity Al plates. The MSR has two-shell structure with a gap distance of 20 cm between the inner wall and the outer wall. The shielding factors as a function of frequency are shown in figure 6. The shielding factors at 0.1 Hz are in the range of 37-40 dB, depending on the directions with maximum value along the door direction. At 10 Hz, the shielding factors are in the range of 72-78 dB, which are large enough for measuring MCG signals.

### F. Operational Characteristics

Figure 7 shows a magnetic field noise spectrum of a gradiometer measured inside the MSR without a subject under the dewar. Including all the noise contributions, such as, dewar thermal noise and the residual magnetic noise of the MSR, the SQUID system noise is about 10 $fT_{rms}/\sqrt{Hz}$ at 1 Hz and 5 $fT_{rms}/\sqrt{Hz}$ at 100 Hz. Figure 8 shows a histogram of the noise distribution for all the 64 channels, measured at 100 Hz. The average value of the noise is 5 $fT_{rms}/\sqrt{Hz}$ at 100 Hz, which is low enough to measure MCG signals with high SNRs. If we simply assume that the noise spectrum is flat with an average noise of 10 $fT_{rms}/\sqrt{Hz}$ in the measuring bandwidth of 0.1-100 Hz, we get a noise amplitude of 100 $fT_{rms}$ or 140 $fT_{peak}$. Thus, we will get an SNR of about 100 for the R-peak of MCG signals.

### G. Dewar Gantry and Bed

To support the He dewar and to adjust the height of the dewar, a manual gantry was fabricated which can be moved vertically using a gear. The patient bed can be moved in two

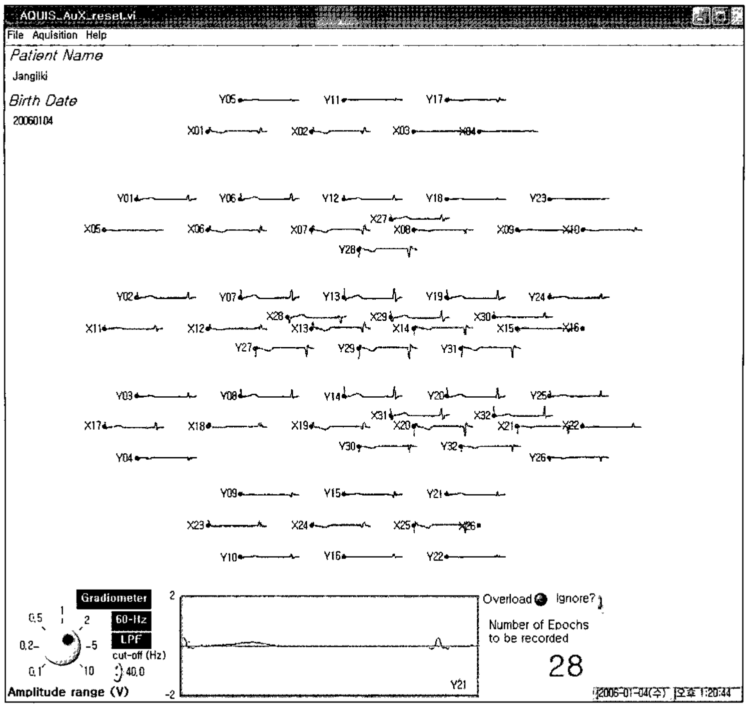


(a)

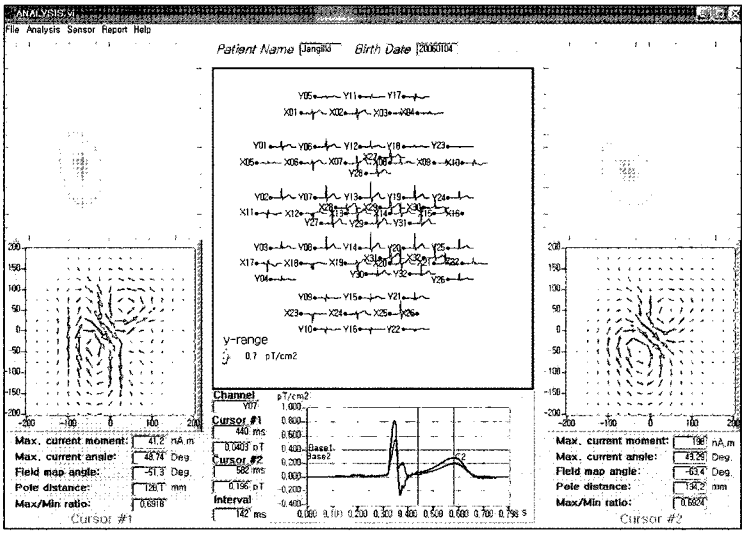


(b)

**Fig. 11.** MCG software. (a) Computer window for the realtime display of an MCG acquisition and (b) analysis window with MCG traces, field maps, current arrow maps, field parameters and current parameters.

horizontal directions using two separate gears and vertically using an oil-pump for the fine adjustment of the measuring positions. The bed has 4 rollers at the bottom legs so that it can be moved along the guide rail on the MSR floor for easy loading of the patients. Figure 9 shows the schematic diagram of the MCG system. All the materials used in the gantry and bed, including gears, were made of nonmagnetic materials. For the fine alignment of patient chests with respect to the dewar, two diode lasers were mounted on the wall of the MSR. The laser beams pass through the reference points of the dewar and cross at the reference point of the subject, xiphoid. A nonmagnetic cycle was installed on the bed for exercise MCG measurements if necessary. Figure 10 shows the photograph of the MCG system installed in a hospital.

## III. MCG MEASUREMENT SOFTWARE

### A. Control and Acquisition

All the controls of the system, acquisition of data and analysis were done with a Window-based personal computer. A 64-channel A/D card (National Instrument, PCI-6033E) of a 16-bit resolution was used for the acquisition of data with a maximum sampling rate of 1.5 kHz. Automatic control of SQUID settings and ASP settings was done through a fiber optic cable. The control software has the functions of optimizing the operation conditions of SQUIDs and heating to remove trapped fluxes. The optimum condition of SQUID settings, such as bias current, voltage offset, flux bias, was determined by the criterion of minimizing the SQUID noise. If there is any channel with a trapped flux in the SQUID or flux transformer, a heating pulse of about 1 W can be applied for 1-3 s duration. Typical MCG measurement time was 30 s. Figure 11(a) shows a window of the realtime display of an MCG measurement. After acquisition of MCG signals, baseline correction, digital filtering, optional averaging and field mapping can be done.

### B. Analysis Software

The analysis sequence of MCG data is different depending the disease; myocardial ischemia or conduction anomaly. Using the minimum-norm estimation method, 2-dimensional myocardium current maps were obtained from the field maps [12]. Based on the information from field maps and current maps, we can calculate the temporal and spatial behavior of the myocardium current parameters, for example, current angle, current moment and current depth, and compared the parameter values between coronary artery disease patients with the normal subjects for the diagnosis of myocardial ischemia.

In case of conduction anomaly, such as WPW syndrome, atrial arrhythmias, and Brugada syndrome, 2-and/or 3-dimensional myocardial current imaging is used to understand the spatial activation behavior of abnormal currents. In localizing the abnormal pathways of WPW syndrome or atrial fibrillation (or flutter), a separative minimum variance beamformer method was developed to reconstruct the myocardial current corresponding to a time-integrated activity for a characteristic waveform. In Brugada syndrome, which is difficult to distinguish from the right bundle branch block, a 2-dimensional-pattern difference in the spatiotemporal activation graph was applied.

## IV. CONCLUSION

We constructed an MCG system having low-noise 64 SQUID planar gradiometers. All the technical elements of the system; SQUID, electronics, dewar, MSR and software were developed and incorporated in the system. The technical features of the system are high intrinsic balancing of the planar gradiometer against external noises, simple FLL electronics owing to high flux-to-voltage transfers of DROSs, low boil-off rate of liquid He dewar, tangential measurements of cardiac fields, accurate classification of myocardial ischemia and localization of conduction anomaly.

Using the developed technology, two MCG systems were constructed and installed in domestic and foreign hospitals, respectively, and measured more than 1000 patients for 2 years. Compared with conventional MCG systems measuring the normal component, the developed MCG system measuring the tangential components with low-noise DROS planar gradiometers could be an economic as well as high-SNR MCG system for the diagnosis of electrophysiology of heart diseases.

## REFERENCES


[1] G. Stroink, W. Moshage, and S. Achenbach, Cardiomagnetism, In: Magnetism in Medicine, W. Andrä and H. Nowak Ed., Berlin: Wiley-VCH, pp.136-189, 1998.

[2] H. Nowak, Biomagnetism, In: Magnetism in Medicine, W. Andrä and H. Nowak Ed., Berlin: Wiley-VCH, pp.85-135, 1998.

[3] J. W. Park, and F. Jung, "Qualitative and Quantitative Description of Myocardial Ischemia by means of magnetocardiography," *Biomed. Technik.*, vol. 49, pp.267-273, 2004.

[4] R. Fenici, D. Brisinda, and A. M. Meloni, "Clinical application of magnetocardiography," *Expert Rev. Mol. Diagn.*, vol. 5, pp.291-313, 2005.

[5] S. Yamada, and I. Yamaguchi, "Magnetocardiograms in clinical medicine: unique information on cardiac ischemia, arrhythmias, and fetal diagnosis," *Internal Medicine*, vol. 44, pp.1-19, 2005.

[6] V. Pizzella, S. D. Penna, C. Del Gratta, and G. L. Romani, "SQUID systems for biomagnetic imaging," *Supercond. Sci. Technol.*, vol. 12, pp.R79-R114, 2001.

[7] D. J. Adelerhof, H. Nijstad, J. Flokstra, and H. Rogalla, "(Double) relaxation oscillation SQUIDs with high flux-to-voltage transfer: Simulations and experiments," *J. Appl. Phys.*, vol. 76, pp.3875-3886, 1994.

[8] Y. H. Lee, H. C. Kwon, J. M. Kim, Y. K. Park, and J. C. Park, "Double relaxation oscillation SQUID with reference junction for biomagnetic multi-channel applications," *Appl. Supercond.*, vol. 5, pp.413-418, 1998.

[9] Y. H. Lee,J. M. Kim, K. Ki, H. Kwon, K. K. Yu, I. S. Kim, and Y. K. park, "64-channel magnetocardiogram system based on

double relaxation oscillation SQUID planar gradiometers," *Supercond. Sci. Technol.*, vol. 19, pp.S284-288, 2006.

[10] J. M. Kim, Y. H. Lee, K. Kim, H. Kwon, Y. K. Park, and I. Sasada, "Compact readout electronics for 62-channels DROS magnetocardiography system," *IEEE Trans. Appl. Supercond.*, vol. 15, pp.644-647, 2005.

[11] K. Kim, Y. H. Lee, H. Kwon, J. M. Kim, I. S. Kim, and Y. K. Park, "Optimal sensor distribution for measuring the tangential field components in MCG," in *Proc. 14th Int. Conf. Biomagnetism Boston*, 2004, pp.359-360.

[12] J. Numminen, S. Ahlfors, R. Ilmoniemi, J. Montonen and J. Nenonen, "Transformation of multichannel magnetocardiographic signals to standard grid form," *IEEE Trans. Biomed. Eng.*, vol. 42, pp.72-78, 1995.